N92-27731

STABILITY AND PERFORMANCE OF NOTCH FILTER CONTROL FOR UNBALANCE RESPONSE

C. R. Knospe
Department of Mechanical and Aerospace Engineering
University of Virginia
Charlottesville, Virginia 22901 USA

May 28, 1991

ABSTRACT

Many current applications of magnetic bearings for rotating machinery employ notch filters in the feedback control loop to reduce the synchronous forces transmitted through the bearings. In this paper, the capabilities and limitations of notch filter control are investigated. First, a rigid rotor is examined with some classical root locus techniques. Notch filter control is shown to result in conditional stability whenever complete synchronous attenuation is required. Next, a nondimensional parametric symmetric flexible three mass rotor model is constructed. An examination of this model for several test cases illustrates the limited attenuation possible with notch filters at and near the system critical speeds when the bearing damping is low. The notch filter's alteration of the feedback loop is shown to cause stability problems which limits performance. Poor transient response may also result. A high speed compressor is then examined as a candidate for notch filter control. A collocated 22 mass station model with lead–lag control is used. The analysis confirms the reduction in stability robustness that can occur with notch filter control. The author concludes that other methods of synchronous vibration control yield greater performance without compromising stability.

NOMENCLATURE

c	derivative feedback coefficient
c_r	rotor damping
$\overline{C}$	nondimensional bearing damping, c/c_r
e_u	unbalance eccentricity
F_b	bearing force
F_u	unbalance force
g	notch gain
H	feedback transfer function
k	proportional feedback coefficient
k_b	open loop magnetic bearing stiffness
k_{eq}	equivalent bearing stiffness
$\overline{K}_{eq}$	nondimensional equivalent bearing stiffness, k_{eq}/k_s
k_s	shaft stiffness

PRECEDING PAGE BLANK NOT FILMED

j	$\sqrt{-1}$
m	rotor mass
m_b	bearing rotor mass
m_d	disk rotor mass
$\overline{M}$	mass ratio, $2m_b/m_d$
N	notch filter transfer function
p	characteristic polynomial
p_e	even part of characteristic polynomial
p_o	odd part of characteristic polynomial
s	complex frequency variable
W	notch width
Z	rotor position
Z_1	complex bearing displacement, $Z_1 = X_1 + j\,Y_1$
Z_2	complex midspan displacement, $Z_2 = X_2 + j\,Y_2$
β	angle from PD zero to notch zero
ϕ	angle from notch pole to notch zero
θ	angle from notch pole to notch zero
ψ	angle of arrival of locus
ζ_d	notch pole damping
ζ_o	notch zero damping
ζ_r	rigid bearing shaft damping, $c_r/2\sqrt{k_s m_d}$
ω_o	operating speed, notch center frequency
$\overline{\omega}$	nondimensional operating speed, ω_o/ω_r
ω_r	rigid bearings critical speed, $\sqrt{k_s/m_d}$
λ	nondimensional complex frequency, s/ω_r

INTRODUCTION

In the last decade, active magnetic bearings for rotating machinery have moved from a promising concept to industrial application. Magnetic bearings have been installed in a variety of machines including pumps and compressors [1,2]. They have been employed successfully in several large rotating machinery applications including over 25 thousand hours of operation on a natural gas pipeline compressor [2]. While these initial experiences with industrial application of magnetic bearings have been encouraging, problems with their installation have been noted. Often, installation of current design of magnetic bearings requires several weeks of "tuning" of the controller [2]. Undoubtedly, as digital control becomes more widespread for magnetic bearings, this time will be shortened. However, the authors believe that the fundamental factor in the long controller installation time is the amount of tuning required to achieve stability and acceptable performance. Better analysis of the rotor dynamic and control issues of a particular application before installation should greatly reduce on–site tuning.

One area that the authors believe has undergone insufficient analysis is the use of notch filters. Many current applications of magnetic bearings have a notch filter in the control feedback loop to suppress rotor synchronous response [3]. The notch frequency is placed at the operating speed and causes the bearings effective stiffness and damping at this speed to be greatly reduced. In principle, the bearings exert little harmonic force upon the rotor and the rotor spins about its inertial axis. Thus, a greatly reduced harmonic force is transmitted to the foundation. However, since the stiffness and damping of the bearings at the rotational speed is very small, the orbits at the bearings may become quite large. The notch filter technique is often referred to as "automatic balancing". This name may be misleading since the reduced bearing stiffness and damping are not analogous to conventional rotor balancing techniques. In conventional rotor balancing, correction weights are added to the shaft so as to reduce the residual unbalance. These weights produce forces which rotate with the shaft counteracting the forces due to the shafts unbalance distribution. Conventional balancing does not change the bearing properties. Thus, conventional balancing does not affect system stability or transient response. Notch filtering changes both these since it alters the bearing properties. With the notch filter, the unbalance distribution about the geometric axis is unaltered; however, the rotor spins about its inertial axis. In theory, the motion of the shaft is not transmitted to the foundation because of the very low stiffness and damping.

Since notch filters achieve synchronous attenuation through altering the magnetic bearing feedback loop, stability becomes an important issue. In practice, the stability issue has a profound impact upon the efficacy of notch filters as a solution to the unbalance response problem. This result has been reported by Beatty [4] for single mass flexible rotors with massless bearings. For the same reason, a notch filter controlled system may also have poor transient response.

The authors emphasize, however, that it is not necessary to use feedback modification to achieve unbalance response attenuation. Because the synchronous response is highly correlated, it can be reduced through an open loop (feedforward) scheme without altering the system transient response or stability. This method has been employed by many researchers [5,6,7,8]. Recently, the authors have demonstrated reductions in transmitted synchronous vibration of 42 dB (over one hundred fold) on an experimental rotor rig [9]. It is interesting to note that, to the authors' knowledge, open loop controllers are currently not in use on any commercial machines. The promise of these controllers will not be discussed further in this paper as the focus remains the examination of notch filter controllers which are widely employed in commercial machines.

In this paper, the stability and performance of notch filter control systems is examined. In Section II, a rigid rotor model is used to introduce the stability and performance issues of notch filter controllers. Section III examines an extended symmetric three mass rotor model and solves for a nondimensionalized characteristic equation and bearing response. In Section IV, the analysis' results are presented and the stability and performance of notch filter controllers is discussed. Section V examines the robustness of a 22 mass station model of a high speed compressor with notch filters in the feedback loop. Section VI closes with conclusions.

II. RIGID ROTOR ANALYSIS

A rigid rotor system with magnetic bearings is discussed here to introduce the instability that can be produced by notch filters in the feedback loop. A rigid rotor in magnetic bearings without stabilizing feedback may be described by a mass, m, attached to a negative spring [10], $k_b < 0$, with a transfer function between bearing force, F_b, and rotor position, Z

$$\frac{Z(s)}{F_b(s)} = \frac{1}{ms^2 + k_b} \tag{1}$$

A block diagram representation is shown in Figure 1. This system has poles at $\pm\sqrt{-k_b/m}$ and is unstable since one pole is in the right half of the complex plane. The system may be stabilized using proportional– derivative (PD) control

$$\frac{F_b(s)}{Z(s)} \equiv H(s) = cs + k \tag{2}$$

resulting in a stable closed loop system transfer function between unbalance force, F_u, and rotor position

$$\frac{Z(s)}{F_u(s)} = \frac{1}{ms^2 + cs + k_{eq}} \tag{3}$$

where $k_{eq} = k_b + k$, if c and k_{eq} are positive. As illustrated in Figure 2, a root locus diagram for the system, the PD control places a zero on the real axis in the left half of the complex plane at $-k/c$. Whether this zero is to the right or left of the pole at $-\sqrt{-k_b/m}$, the system will be stabilized provided $k > -k_b$. The bearing of the closed loop system will have equivalent stiffness k_{eq} and damping c.

The transfer function for a simple notch filter centered at the operating speed ω_o, characterized by its gain, g, and its width, W, is

$$N(s) = \frac{s^2 + 2\zeta_o\omega_o s + \omega_o^2}{s^2 + 2\zeta_d\omega_o s + \omega_o^2} \tag{4}$$

$$g = \frac{\zeta_o}{\zeta_d} \qquad W = 2\zeta_d\omega_o \tag{5}$$

where ζ_o and ζ_d are the damping of the notch filter zeros and poles respectively. The notch gain g is the gain of a signal at frequency ω_o as it passes through the notch. The notch depth, D, $D = 1 - g$, specifies the amount of signal rejected at ω_o. Note that if the notch gain is zero then a signal at ω_o is completely removed by the filter. If the notch gain is one then the signal is completely passed. The notch width is the width of the frequency band where attenuation is greater than –3dB when the notch depth is one [4]. Figure 3 shows the magnitude plot of notch filters of various depths and widths.

A notch filter may be placed in the magnetic bearing feedback loop in essentially two fashions: (1) directly in serial with the PD control, and (2) in serial with PD control after the plant has been compensated for its negative bearing stiffness. In the first case, the controller transfer function is

$$\frac{F_b(s)}{Z(s)} \equiv H(s) = (cs + k)\, N(s) \tag{6}$$

and in the second case

$$\frac{F_b(s)}{Z(s)} \equiv H(s) = -k_b + (cs + k_{eq})\, N(s) \tag{7}$$

In the first case, if the notch has a gain

$$g < -k_b/k$$

then the system will have a negative stiffness to vibrations at ω_o and will therefore be unstable. In the second case, the notch gain would have to be negative to produce an effective negative stiffness at frequency ω_o. Since it is simpler for explanation and no generality is lost, only the second case will be examined in this paper.

When the notch gain is zero, the bearings have no synchronous stiffness or damping and no synchronous vibration is transmitted to the foundation. In practice, however, k_b cannot be known precisely and one cannot cancel it exactly using feedback. It is likely that the bearings after this compensation would have some equivalent stiffness. This would limit the ability of the notch filter to attenuate the transmitted vibration. Thus, the assumption that k_b can be precisely canceled will yield the ideal performance for the notch filter. This ideal case is examined here since the problems associated with notch filters, as will be shown, are serious enough that even their idealized performance will discourage their continued use.

After feedback compensation for the negative bearing stiffness, the plant (rotor plus stabilizing stiffness $-k_b$) has the transfer function

$$\frac{Z(s)}{F_b(s)} = \frac{Z(s)}{F_u(s)} = G(s) = \frac{1}{ms^2} \tag{8}$$

and the notch filter feedback controller has the transfer function

$$H(s) = (k_{eq} + cs)\, N(s) \tag{9}$$

The plant has two poles at the origin of the complex plane while the controller has poles at

$$-\zeta_d\omega_o \pm j\omega_o\sqrt{1 - \zeta_d^2}$$

and zeros at

$$-\frac{k_{eq}}{c}\ , \quad -\zeta_o\omega_o \pm j\omega_o\sqrt{1 - \zeta_o^2}$$

If the notch gain is zero ($\zeta_o = 0$) then the complex zeros of GH are on the imaginary axis. If the notch width is 20% of ω_o ($\zeta_d = 0.1$), a possible pole–zero structure and root locus is shown in Figure 4. Note that two closed loop poles are in the right half complex plane and the system is unstable. Even though the poles of the notch filter are placed near the zeros, the loci stray into the right half plane.

Interestingly, the conditional stability of zero notch gain controllers can be examined through the classical root locus technique of the angle of arrival. The angle of arrival is the angle in the complex plane at which a locus approaches an open loop zero. Evans [9] first established that the sum of the angles from the open loop poles of the system to a point on a locus minus the sum of the angles from the open loop zeros to the same point must be 180°. From this, it is easy to calculate the angle of arrival of a locus at a zero. For the example, the loci must approach the imaginary zeros from the left to ensure unconditional stability. Thus, their angles of arrival must be between 90° and 270°. Given that the notch is thin ($\zeta_d << 1$), this yields a condition for stability of these roots in terms of the angle from the PD zero on the negative real axis to the open loop imaginary zero, β:

$$90^\circ < \beta < 270^\circ$$

Clearly, this condition is only satisfied when the zero on the real axis is in the right half plane. Thus, for a given ratio of equivalent stiffness to damping (which would be chosen by the designer for transient response since this determines the log decrement) the closed loop system with notch filter will go unstable as the stiffness is increased.

Indeed, it is easy to show that conditional stability of this kind will always result if the notch gain is zero for any notch width. Figure 5 illustrates the argument. Note that for any notch filter of the form Eqn. (4), the poles and zeros lie along a semi–circle of radius ω_0 in the left half plane. From geometry, the angle from any possible notch pole circumscribing the two undamped zeros is right (i.e. $\phi + \theta = 90^\circ$). The angles from the open loop poles to a point on the locus as it arrives at the notch zero are ϕ, θ, 90°, and 90°. The angles from the open loop zeros to the point are ψ, β, and 90° where ψ, the angle of arrival, must satisfy

$$90^\circ < \psi < 270^\circ$$

for unconditional stability. The angle of arrival condition

$$(\phi + \theta + 90^\circ + 90^\circ) - (\psi + \beta + 90^\circ) = 180^\circ$$

with $\phi + \theta = 90^\circ$, yields

$$-\psi = \beta$$

and

$$90^\circ < \beta < 270^\circ$$

This establishes that conditional stability will always occur if the PD control zero is placed on the negative real axis (i.e., damping and stiffness are positive). Conditional stability can only be eliminated by having a notch gain greater than zero. However, as the notch is made more shallow, the attenuation of the transmitted synchronous vibration is reduced.

This conditional stability is not surprising since the notch filter introduces phase lag at frequencies below the center frequency. Thus, the feedback controller may not have phase lead at the rotor natural frequencies, resulting in instability.

III. FLEXIBLE ROTOR MODEL

A symmetric three mass rotor model with flexible shaft and notch filter controller is examined in this section. The model to be used, shown in Figure 6, is described by the Laplace domain dynamical equations

$$\begin{aligned}&[m_b s^2 + \tfrac{1}{2} k_s + k_b + H(s)]\, Z_1(s) = [\tfrac{1}{2} k_s]\, Z_2(s)\\ &[m_d s^2 + c_r s + k_s]\, Z_2(s) = [k_s]\, Z_1(s) + F_u(s)\end{aligned} \tag{10}$$

where m_b is the rotor bearing mass, m_d is the rotor disk mass, c_r is the rotor damping, k_s is the shaft stiffness, $Z_1(s)$ is the complex displacement at the bearing, $Z_2(s)$ is the complex displacement at midspan, H(s) is the controller transfer function, and $F_u(s)$ is the unbalance force which is assumed to act at the midspan. The feedback controller transfer function is given by

$$H(s) = -k_b + (cs + k_{eq})\, N(s) \tag{11}$$

where N(s) is the notch filter transfer function defined in Eqn. (4). The characteristic equation for this system is given by

$$0 = [m_b s^2 + \tfrac{1}{2} k_s + k_b + H(s)]\, [m_d s^2 + c_r s + k_s] - \tfrac{1}{2} k_s^2 \tag{12}$$

With the nondimensional quantities ω_r, ζ_r, $\overline{M}$, $\overline{C}$, $\overline{K}_{eq}$, and $\overline{\omega}$ defined in the nomenclature, the characteristic polynomial, Eqn. (12), becomes

$$\begin{aligned}0 = \;& [\tfrac{1}{2} \overline{M}\, \lambda^2 + \tfrac{1}{2}][\lambda^2 + 2\zeta_r\lambda + 1][\lambda^2 + 2\zeta_d\overline{\omega}\lambda + \overline{\omega}^2]\\ &+[2\overline{C}\zeta_r\lambda + \overline{K}_{eq}][\lambda^2 + 2\zeta_r\lambda + 1][\lambda^2 + 2\zeta_o\overline{\omega}\lambda + \overline{\omega}^2]\\ &-\tfrac{1}{2}[\lambda^2 + 2\zeta_d\overline{\omega}\lambda + \overline{\omega}^2]\end{aligned} \tag{13}$$

where λ is the nondimensional complex frequency, $\lambda = s/\omega_r$. This is a sixth order polynomial in λ which defines the closed loop poles of rotor–controller system,

$$p(\lambda) = p_6\, \lambda^6 + p_5\, \lambda^5 + p_4\, \lambda^4 + p_3\, \lambda^3 + p_2\, \lambda^2 + p_1\, \lambda + p_0 \tag{14}$$

where the coefficients are defined by

$$p_6 = \overline{M}/2$$

$$p_5 = \overline{M}\zeta_d\overline{\omega} + \overline{M}\zeta_r + 2\zeta_r\overline{C}$$

$$p_4 = \tfrac{1}{2}\overline{M}\,\overline{\omega}^2 + 2\overline{M}\zeta_r\zeta_d\overline{\omega} + \tfrac{1}{2}(\overline{M}+1) + 4\zeta_r\zeta_o\overline{C}\,\overline{\omega} + 4\zeta_r^2\overline{C} + K_{eq}$$

$$\begin{aligned} p_3 = {} & \overline{M}\,\zeta_r\overline{\omega}^2 + (\overline{M}+1)\,\zeta_d\overline{\omega} + \zeta_r + 2\zeta_r\overline{C}\,\overline{\omega}^2 + 2\zeta_r\overline{C} + 2\zeta_r K_{eq} \\ & + 2(4\zeta_r^2\,\overline{C} + K_{eq})\,\zeta_o\,\overline{\omega} \end{aligned} \tag{15}$$

$$\begin{aligned} p_2 = {} & \tfrac{1}{2}(\overline{M}+1)\,\overline{\omega}^2 + 2\zeta_r\zeta_d\overline{\omega} + (4\zeta_r^2\,\overline{C} + K_{eq})\,\overline{\omega}^2 \\ & + 4(\overline{C} + K_{eq})\,\zeta_r\zeta_o\,\overline{\omega} + K_{eq} \end{aligned}$$

$$p_1 = \zeta_r\,\overline{\omega}^2 + 2(\overline{C} + K_{eq})\,\zeta_r\,\overline{\omega}^2 + 2\,K_{eq}\,\zeta_o\,\overline{\omega}$$

$$p_0 = K_{eq}\,\overline{\omega}^2$$

The unbalance force transmitted through the bearings to the foundation is, in terms of the nondimensionalized parameters,

$$\frac{F_b(\lambda)}{me_u\omega_r^2} = \frac{[2\zeta_r\,\overline{C}\lambda + K_{eq}]\quad N(\lambda)\,\overline{\omega}^2}{[\overline{M}\lambda^2+1 + 2(2\zeta_r\overline{C}\lambda + K_{eq})\;N(\lambda)][\lambda^2 + 2\zeta_r\lambda+1] - 1} \tag{16}$$

Using the coefficients of the characteristic polynomial, an efficient procedure may be employed for finding the largest stabilizing notch depth as a function of the nondimensionalized parameters ζ_o, ζ_r, $\overline{C}$, K_{eq}, $\overline{\omega}$ and $\overline{M}$.

For a system to be stable, the roots of its characteristic polynomial must all lie in the left half of the complex plane. Polynomials satisfying this condition are called Hurwitz [11,12]. A method for determining the lowest possible notch gain for a stable rotor system is to continually check a Hurwitz stability condition as ζ_o is decreased starting with ζ_o equal to ζ_d (no notch filter). When the notch filter is absent from the feedback loop, the rotor system will be stable if $\overline{C}$ and K_{eq} are positive. As the notch is made deeper for a given bearing ($\overline{C}$, K_{eq}), the closed loop poles will move continuously in the complex plane. When the notch becomes of sufficient depth, a complex pole will enter the right half plane. On a Nyquist plot, this will appear as a clockwise encirclement of the critical point, as discussed in Beatty [4]. As the notch becomes deeper, the encirclement will remain. Thus, the range of notch gains between zero and one is divided into a stable and an unstable interval.

IV. SIMPLE MODEL RESULTS

In this section, the degree of attenuation of synchronous transmitted force obtainable with a notch filter controller is examined. This is done to explore the limits of notch filters and not to suggest an actual method of implementation. Thus, while we show the attenuation possible over an entire speed range, we are not suggesting that this is in practice desirable or implementable.

Given the nondimensional parameters for the rotor ($\overline{M}$, ζ_r), the control ($\overline{C}$, K_{eq},

ζ_d), and the operating speed ($\overline{\omega}$), the notch of greatest possible depth (ζ_o) that may be employed while preserving system stability may be found by repeatedly checking stability. From the notch depth so determined, the magnitude of synchronous bearing force can be calculated using Eqn. (16). This is the minimum transmitted force due to unbalance that can be obtained using a notch filter in the feedback loop. (It is easy to demonstrate that maximizing notch depth minimizes transmitted force.) In cases with non–zero notch gain, the system has only marginal stability. In this case, a pair of poles lies along the imaginary axis. Thus, any transient to this system will cause it to 'ring' at this frequency. The only way to amend this undesirable behavior is to reduce the notch depth and thus the synchronous attenuation obtained. Note that in practice the degree of synchronous response attenuation indicated in this analysis cannot be obtained; any implemented feedback controller must have some stability margin.

The analysis was conducted for a three disk magnetic bearing rotor rig used at the University of Virginia. This rig has been used in various research projects and is well characterized [10,13,14]. The nominal values of the nondimensional parameters are

$$\overline{M} = 1.466 \qquad \zeta_r = 0.0625$$
$$\overline{C} = 10.5 \qquad K_{eq} = 0.906$$
$$\zeta_d = 0.10 \quad (\text{Width} = 20\%\ \omega_o)$$

Figure 7 shows the theoretical non–dimensional transmitted synchronous force (without notch filtering) as a function of nondimensional operating speed $\overline{\omega}$ and nondimensional bearing damping $\overline{C}$. Note the two separate critical speeds at low damping. The limit imposed by stability to the attenuation of this synchronous transmitted force are now examined.

In Figure 8 the minimum notch gain that may be employed while maintaining stability is shown as a function of operating speed and damping. A very deep notch can be obtained above the first critical speed if a high degree of bearing damping is employed. However, if the bearing damping is less than five times the rotor damping, a notch in the region of the second critical cannot be 20 dB deep (gain of 0.1). To achieve this depth at the first critical, the bearing damping must be approximately twenty times the rotor damping. Unfortunately, the synchronous vibration problem is greatest at the critical frequencies where the notch must be the shallowest to maintain stability. In design of PD control for magnetic bearings, the damping is chosen to yield good transient performance and robustness to unmodeled destabilizing forces. It is not desirable to set the bearing damping so as to permit the use of a notch filter.

Figure 9 shows the minimum synchronous bearing force that can be achieved with a notch filter controller at each operating speed as a function of bearing damping. The notch employed at each operating speed and damping is the deepest that may be used with system stability maintained. As Figure 8 suggests, the attenuation of notch filter control when the bearing damping is light is poor near the rotor criticals, approximately 6 dB as can be seen in comparing Figures 7 and 9. When the nondimensional rotor damping is above 10, 20 dB (factor of 10) attenuation can be obtained at any operating speed.

Figure 10 shows the nondimensional bearing force (without notch) for the same three mass rotor model as before except that the bearing masses have been reduced to one quarter the midspan disk mass ($\overline{M} = 0.5$). Thus, this model acts more like a single mass rotor. Note that the second critical speed is significantly higher. Figure 11 shows the minimum stabilizing notch gain as a function of the nondimensional rotational frequency and damping. Note that the range of operating speeds at low damping near the second critical speed requiring shallow notch filters is much broader than with the first rotor examined (Figure 8). Interestingly, the maximum transmitted force with the notch filter, Figure 12, does not occur at the same frequency as the second critical (without notch) or where the notch is the shallowest. While this seems counter–intuitive, the introduction of the notch filter alters the location of the closed loop poles in the complex plane. As discussed by Dorf [15], the synchronous response of a system is inversely proportional to the distance of the poles from the synchronous frequency on the imaginary axis. Thus, the maximum synchronous response of a synchronous notch system will not occur at the critical frequency of the system without notch since the closed loop pole locations have been altered by the introduction of the notch.

The author wishes to emphasize that the performance indicated here is ideal since it has been assumed that the unstable bearing stiffness can be precisely canceled through feedback and that notch filter controller–rotor system can operate without any stability margin. It should also be pointed out that the notch controller–rotor systems represented that are marginally stable possess a pole on the imaginary axis. Therefore, any disturbance acting at this asynchronous frequency will result in very large displacements.

V. ROBUSTNESS ANALYSIS

We now examine a more realistic rotor model to gauge the effect of notch filters on magnetic bearing system robustness. The 'rotor' employed for this analysis is a 22 mass station model of a high speed test rig constructed at the University of Virginia to simulate an aircraft compressor [16]. The designed operating speed range of this machine is 30,000 to 70,000 rpm. The model employs collocated sensors and actuators and local lead–lag control. The negative bearing stiffness is assumed to have been compensated. The magnetic bearings and the sensors are assumed to have infinite bandwidth. Gyroscopic terms are not included in the model. These assumptions were made so that the results are easier to analyze. We may fairly attribute changes in robustness with the introduction of notch filters to the notch filters themselves and not to the notch filters' interaction with other destabilizing mechanisms (e.g. non–collocation). The rotor with bearing locations is shown in Figure 13.

The structured singular value method is used to analyze the magnetic bearing system robustness with notch filters. Multiplicative uncertainty elements (Δ_1, Δ_2) are placed in the feedback path as shown in Figure 14. These uncertainties are complex numbers and therefore represent some gain and phase change to the signals in the feedback loop. A notch filter operating speed is fixed and the structured singular values of this plant (rotor, phase lead control, notch filters) with respect to the multiplicative uncertainty is computed [17]. The structured singular value is the inverse of the size of the smallest complex uncertainty matrix $\Delta = \text{diag}(\Delta_1, \Delta_2)$ which destabilizes the system. Thus, the structured singular value can be thought of as the inverse of the gain/phase margin at each frequency. Large structured singular values in a frequency range indicates poor stability robustness to unmodeled dynamics in this frequency band.

In this analysis, the maximum structured singular values over frequency is found for the rotor system with and without notch filters. This serves as our robustness measure. We examine this measure as a function of the center frequency of the notch filter. Robustness is therefore examined as a function of notch filter/rotor operating speed much as in Section IV.

In the first analysis, a narrow notch with a notch gain of 0.1 is used. Figure 15 shows the maximum structured singular value as a function of notch center frequency. Also shown is the maximum structured singular value for the system without notch filters. Note that the maximum structured singular value ("mu") is highest in the region of the rotors critical speeds without notches (first critical: 5530 rpm; second: 10910 rpm; third: 22350 rpm; fourth 55800 rpm). Thus, if a notch filter with 20 dB attenuation were used on this rig near one of these speeds, the system would be much more prone to destabilization due to uncertainties in each feedback loop. The use of notch filters in this operating speed range will make the rotor system much more sensitive to components in the feedback loop (sensors, filters, amplifiers, and actuators). This may help to explain the difficulties experienced in "tuning" magnetic bearing systems.

The maximum structured singular value can be converted to either gain margin or phase margin specifications. These margins are guaranteed margins; that is the system will be stable for at least the amount of variation specified by the margin. Because the system we are examining is a resonant system (which is always stabilized by collocated phase–lead control), closed loop stability is much more sensitive to phase changes. Thus, it is reasonable to expect that the actual multivariable phase margin is not much greater than the guaranteed phase margin specified by the maximum structured singular value. Figure 16 shows the guaranteed phase margin as a function of notch center frequency. Note that without notch filters, the system has 41° phase margin. However, with a notch filter included, the phase margin drops considerably, especially near critical speeds. It should be noted that most control systems are designed to have phase margins greater than 20°. In the author's opinion, a healthy phase margin is necessary for a properly running magnetic bearing system.

This analysis was also carried out with a notch filter with 40 dB depth. The maximum structured singular value as a function of notch center frequency for this case is shown in Figure 17. Below approximately the third critical speed the rotor is unstable (without any multiplicative uncertain). As the notch center frequency is increased, the system becomes less sensitive to phase/gain changes in the feedback loops. Figure 18 shows the corresponding guaranteed phase margin of the system with and without notch filters as a function of notch center frequency. Note that at no frequency in the rotors operating speed range will the system with notch filters have a phase margin of 20°.

VI. CONCLUSIONS

Analysis of synchronous notch filter controllers for unbalance response attenuation of magnetically suspended rotors demonstrates that the introduction of a notch filter into the feedback loop has a profound affect on system stability and robustness. It was shown that for a rigid rotor complete attenuation was impossible without conditional stability. For flexible rotors, notch depth was restricted by instability near the critical speeds. If the bearing damping is low, transmitted force attenuation is small near the critical speed. When set for a given operating speed, asynchronous disturbances can cause large displacements since the notch filter controlled rotor may be marginally stable. This is an important consideration for practical rotor systems which have subharmonic excitations due to cross coupled effects such as seals. Structured singular value analysis was used to show the reduced robustness that may occur when notch filters are introduced into the feedback loop. This analysis examined the robustness with respect to the simultaneous inependent gain/phase changes in each loop. Notch filter controllers may also have poor robustness to changes in the rotor (for example, thermal induced changes in Young's modulus) and destabilizing fluid forces which are not representable by this structure.

Due to these problems with notch filter controllers, the author strongly recommends that magnetic bearing users employ open loop (feedforward) control strategies for synchronous vibration reduction. These controllers have been demonstrated by many researchers to yield superior vibration attenuation with no stability problems.

REFERENCES

[1] Imlach, J., Humphris, R., Blair, B., Allaire, P., and Lewis, D., "Testing of a Magnetic Bearing Equipped Canned Motor Pump for Installation in the Field," 2nd International Symposium on Magnetic Bearings, Tokyo, Japan, July 12–14, 1990, pp. 39–45.

[2] Foster, E., Kulle, V., and Peterson, R., "The Application of Active Magnetic Bearings to a Natural Gas Pipeline Compressor," ASME Paper 86–GT–1, presented at International Gas Turbine Conference and Exhibit, Dusseldorf, West Germany, June 8–12, 1986.

[3] Haberman, H. and Brunet, M., "The Active Magnetic Bearing Enables Optimum Damping of Flexible Rotors," ASME Paper 84–GT–117, 1984.

[4] Beatty, R., "Notch Filter Control of Magnetic Bearings to Improve Rotor Synchronous Response", Master's Thesis, MIT, May 1988.

[5] Burrows, C.R., Sahinkaya, N., Traxler, A., and G. Schweitzer, "Design and Application of a Magnetic Bearing for Vibration Control and Stabilization of a Flexible Rotor," Proceedings of the First International Symposium on Magnetic Bearings, ETH Zurich, Switzerland, June 6–8, Springer–Verlag, 1988.

[6] Higuchi, T., Mizuno, T., and Tsukamoto, M., "Digital Control System for Matnetic Bearings with Automatic Balancing," Proceedings of the 2nd International Symposium on Magnetic Bearings, Tokyo, Japan, July 12–14, 1990.

[7] Kanemimtsu, Y., Ohsawa, M., and Watnabe, K., "Real Time Balancing of a Flexible Rotor Supported by Magnetic Bearings," Proceedings of the 2nd International Symposium on Magnetic Bearings, Tokyo, Japan, July 12–14, 1990.

[8] Nonami, K., and Kawamata, S., "Feedforward Control to Unbalance Force Cancellation for Flexible Rotor Systems," Proceedings of the International Symposium on Advanced Computers for Dynamics and Design (ACD&D), Tsuchiura, Japan, Sept. 6–8, 1989.

[9] Knospe, C.R., Humphris, R.R., and Sundaram, S., "Flexible Rotor Balancing using Magnetic Bearings," Proceeding of the Conference on Recent Advances in Active Control of Sound and Vibration, Blacksburg, VA., April 15–17, 1991. Techomics Publishing, Lancaster, PA, pp. 420–429, 1991.

[10] Humphris, R., Allaire, P., Lewis, D., and Barrett, L., "Diagnostic and Control Features with Magnetic Bearings," Proc. of the 24th Intersociety Energy Conversion Engineering Conference, Washington, D.C., August 6–11, 1989, pp. 1491–1498.

[11] Evans, W., <u>Control–System Dynamics</u>, McGraw–Hill, New York, 1954, pp. 96–121.

[12] Bhattacharyya, S. P., <u>Robust Stabilization Against Structured Perturbations</u>, Lecture Notes in Control and Information Sciences, Vol. 99, Springer Verlag, Berlin, 1987, pp. 14–22.

[13] Humphris, R., Kelm, R., Lewis, D., and Allaire, P., "Effect of Control Algorithms on Magnetic Journal Bearing Properties," Journal of Engineering for Gas Turbines and Power, Vol. 108, Oct. 1986, pp. 624–632.

[14] Williams, R., Keith, F., and Allaire, P., "Digital Control of Active Magnetic Bearings," IEEE Transactions on Industrial Electronics, Vol. 37, No. 1, February 1990, pp. 19–27.

[15] Dorf, R., Modern Control Systems, Addison–Wesley, Reading, MA, 1967, pg. 190.

[16] Maslen, E., Allaire, P., Scott, M., and Herman, P., "Magnetic Bearing Design for a High Speed Rotor,"

[17] Doyle, J.C., "Analysis of Feedback Systems with Structural Uncertainties", IEE Proceedings, Part D., Volume 129, No. 6, pp. 242–250, Nov. 1982.

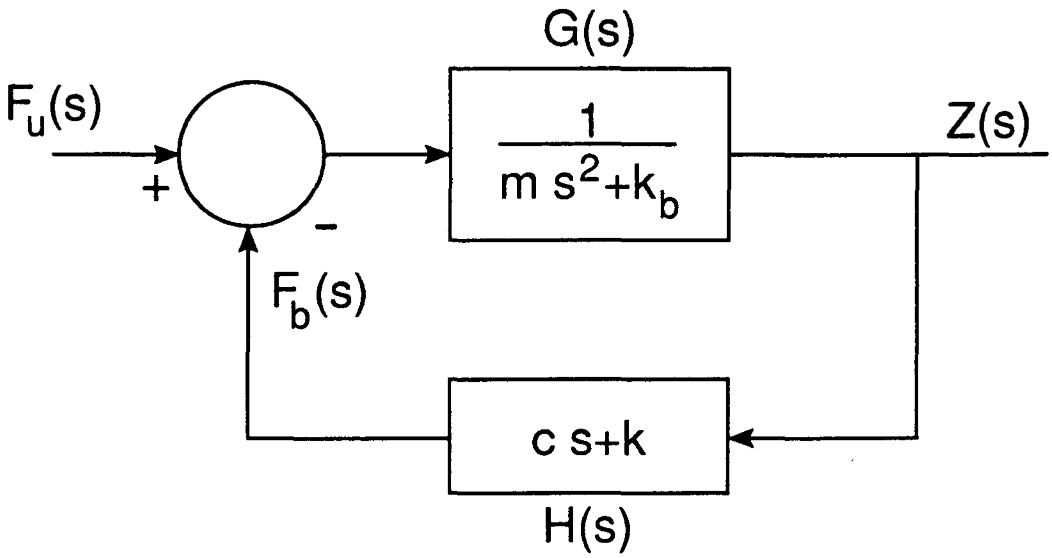

Figure 1: Block diagram of rigid rotor system in magnetic bearings

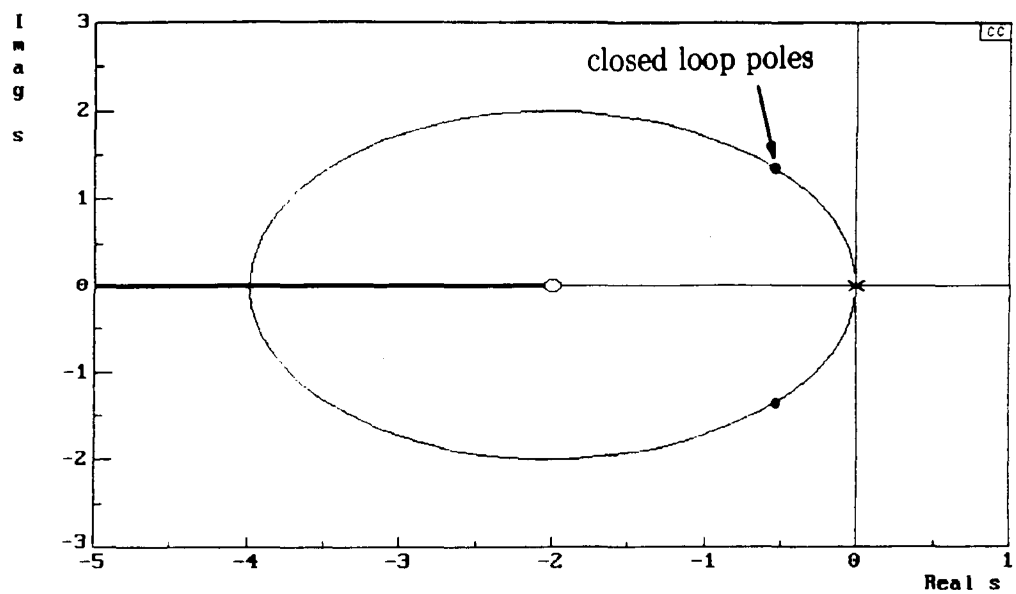

Figure 2: Root locus for PD control of a rigid rotor

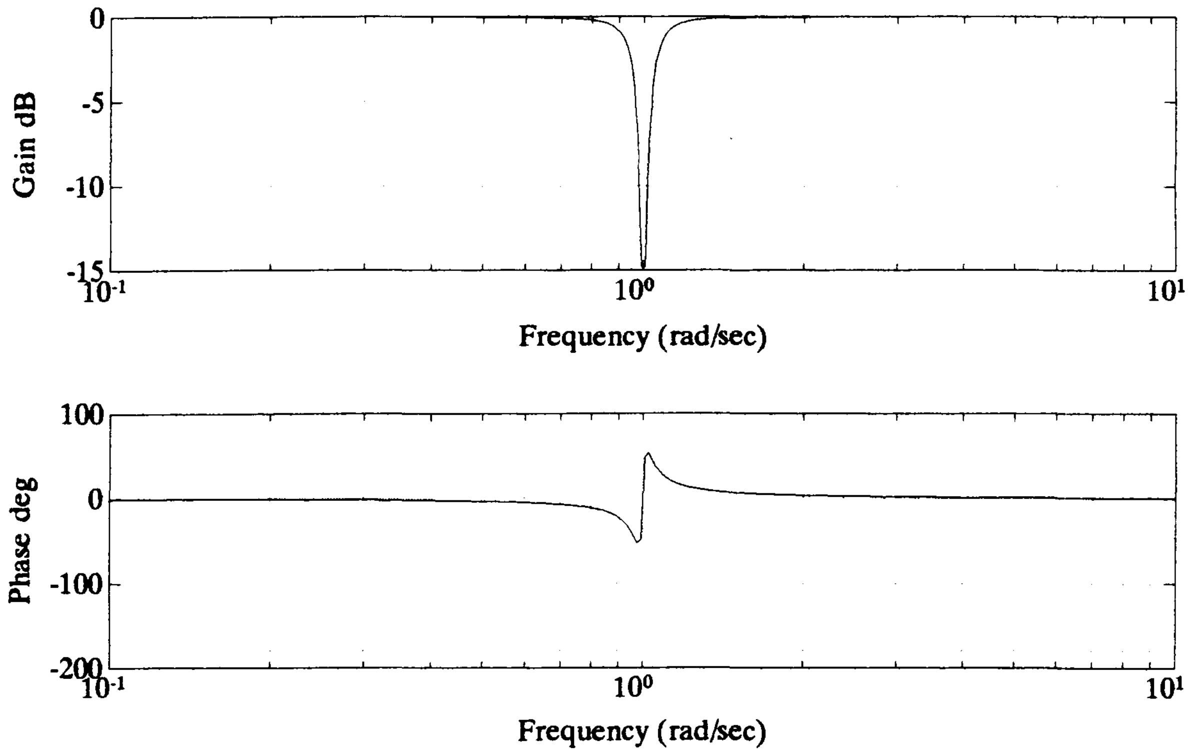

Figure 3: Notch filter magnitude plots

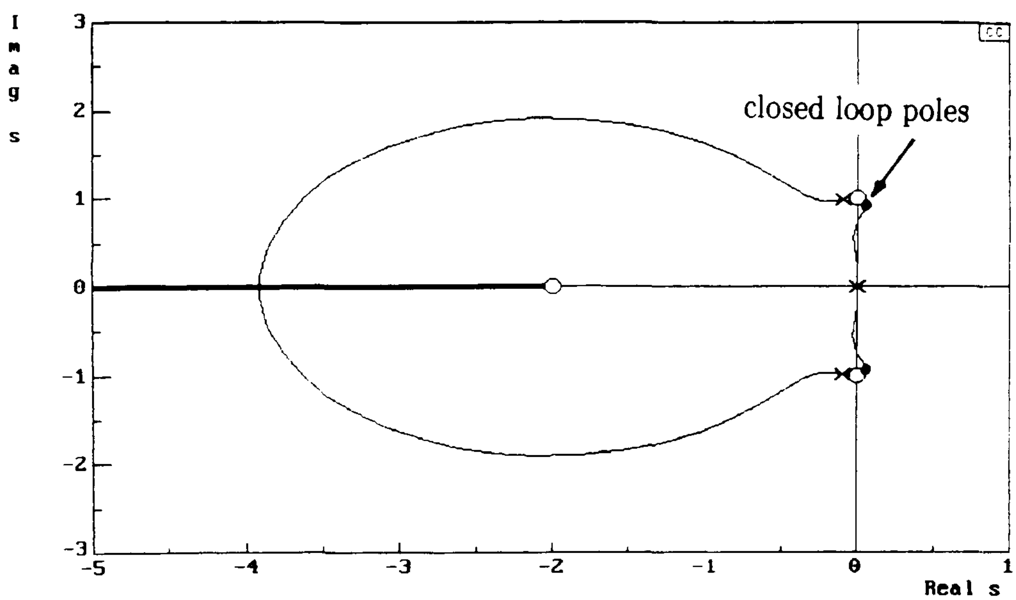

Figure 4: Root locus for notch filter–PD control of a rigid rotor ($\zeta_o = 0$, $\zeta_d = 0.1$)

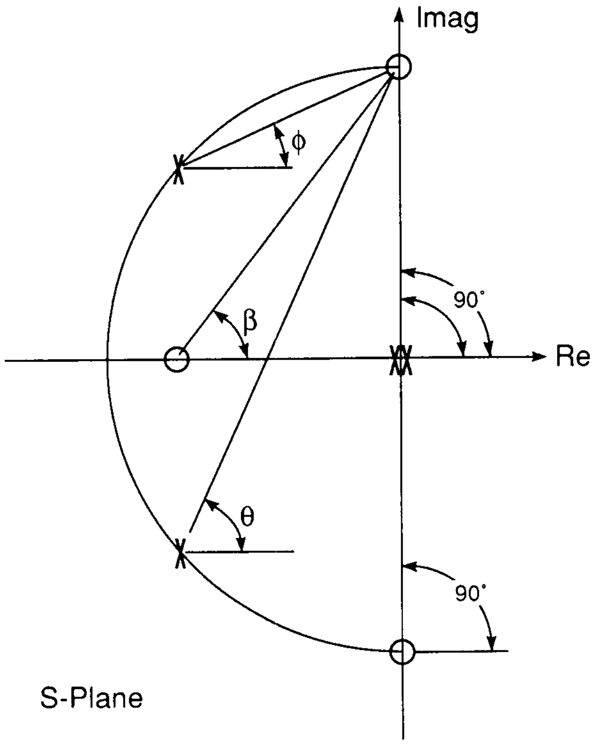

Figure 5: Locus angle for arrival condition ($\zeta_o = 0$, $\zeta_d \leq 1$)

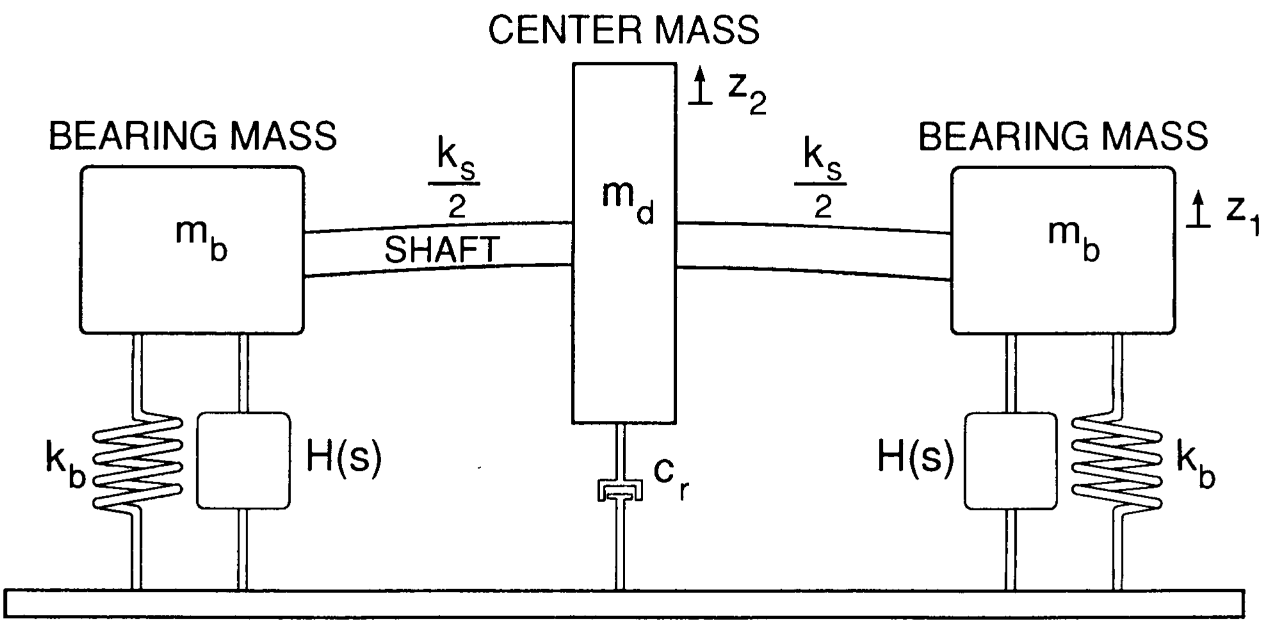

Figure 6: Symmetric three mass rotor model

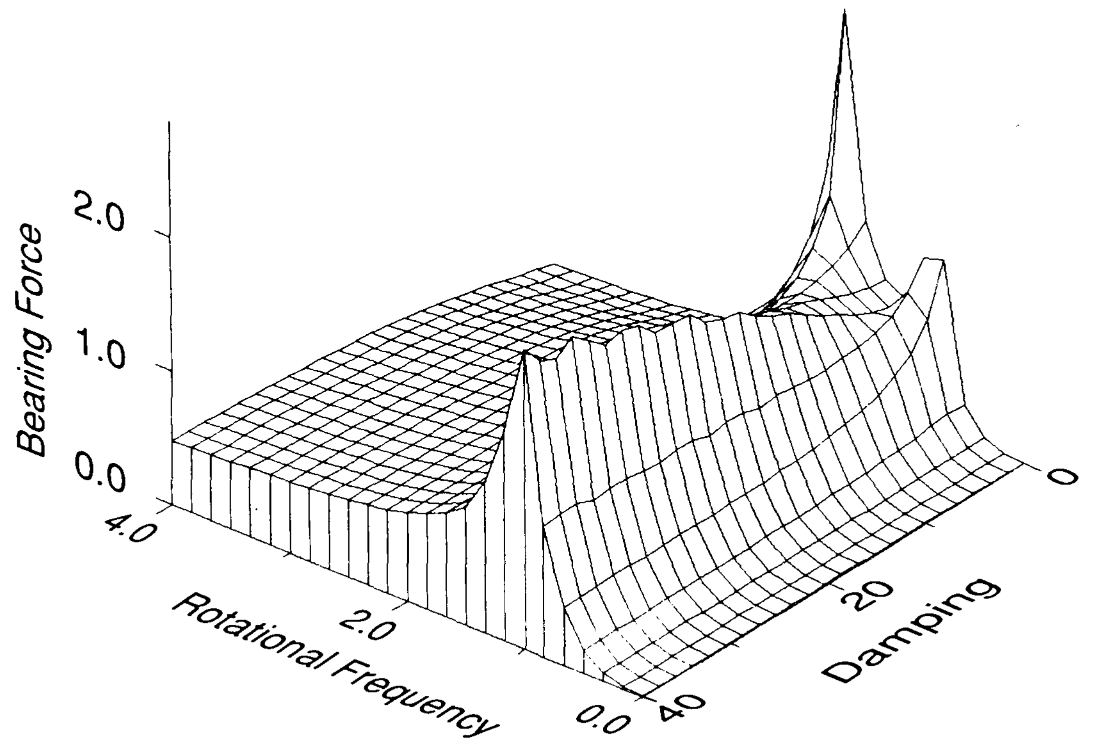

Figure 7: Nondimensional transmitted synchronous force at each nondimensional operating speed as a function of nondimensional bearing damping ($\overline{M} = 1.466$, $\zeta_d = 0.1$)

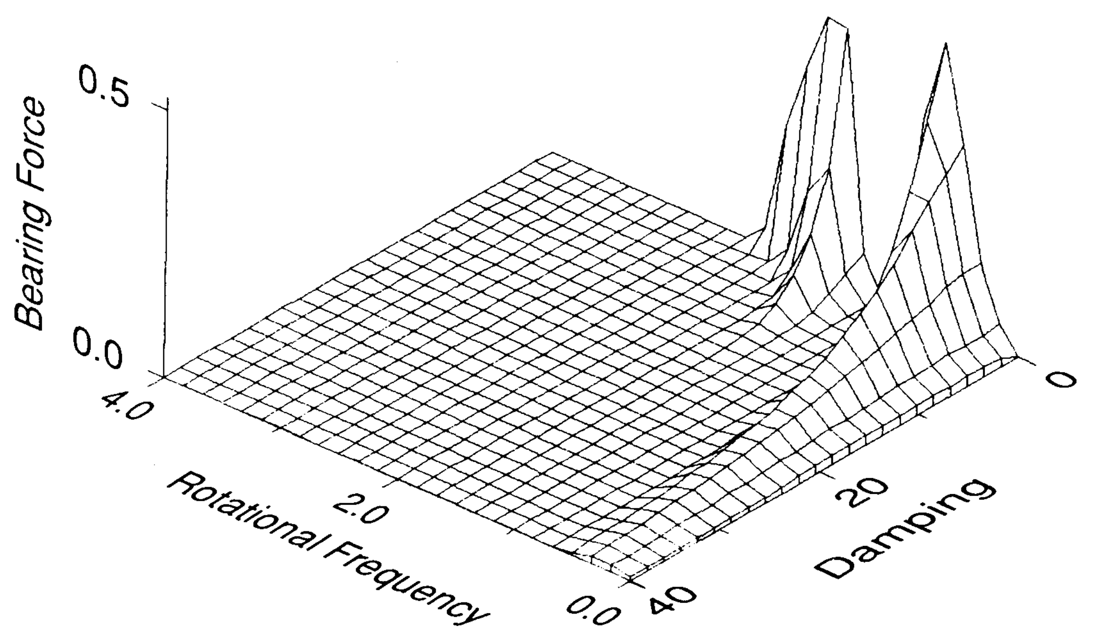

Figure 8: Minimum notch gain at each nondimensional operating speed as a function of nondimensional bearing damping ($\overline{M} = 1.466$, $\zeta_d = 0.1$)

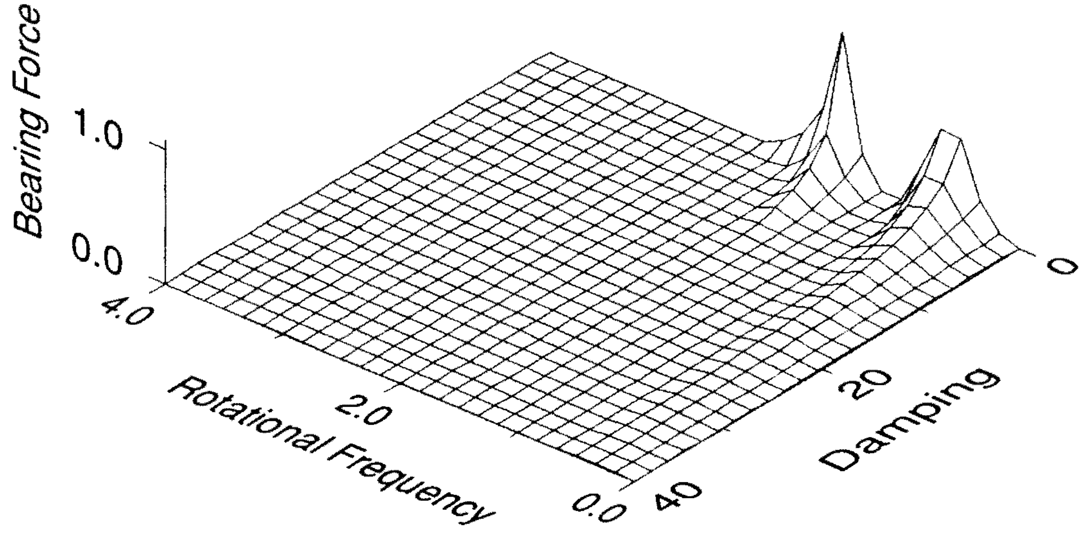

Figure 9: With notch filter control: Nondimensional transmitted synchronous force at each nondimensional operating speed as a function of nondimensional bearing damping ($\overline{\mathrm{M}} = 1.466$, $\zeta_d = 0.1$)

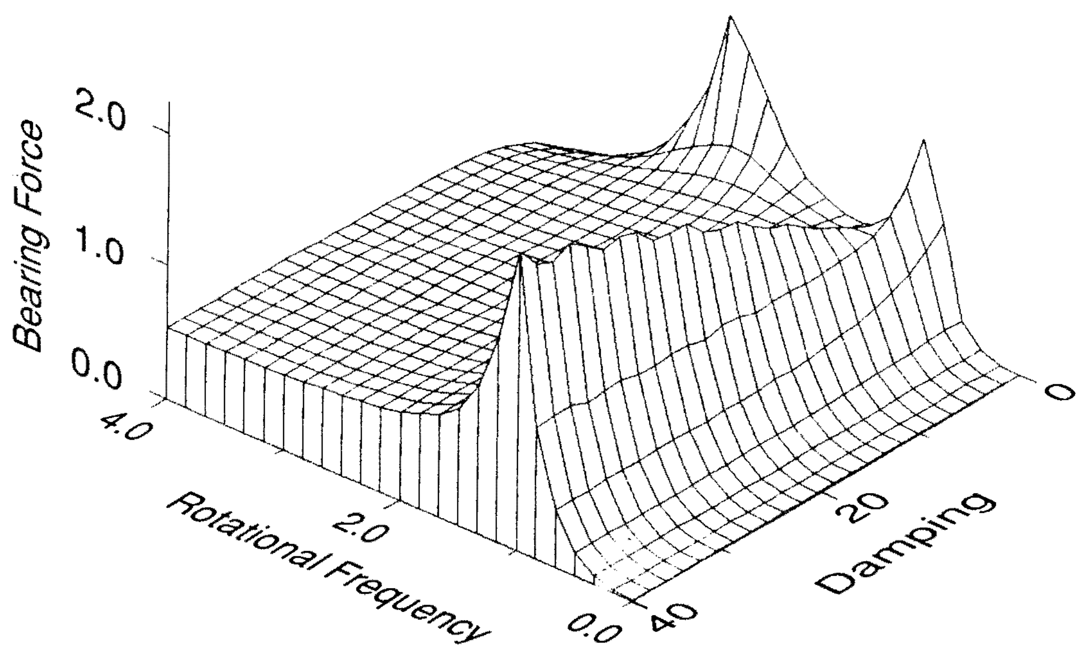

Figure 10: Nondimensional transmitted synchronous force at each nondimensional operating speed as a function of nondimensional bearing damping ($\overline{\mathrm{M}} = 0.5$, $\zeta_d = 0.1$)

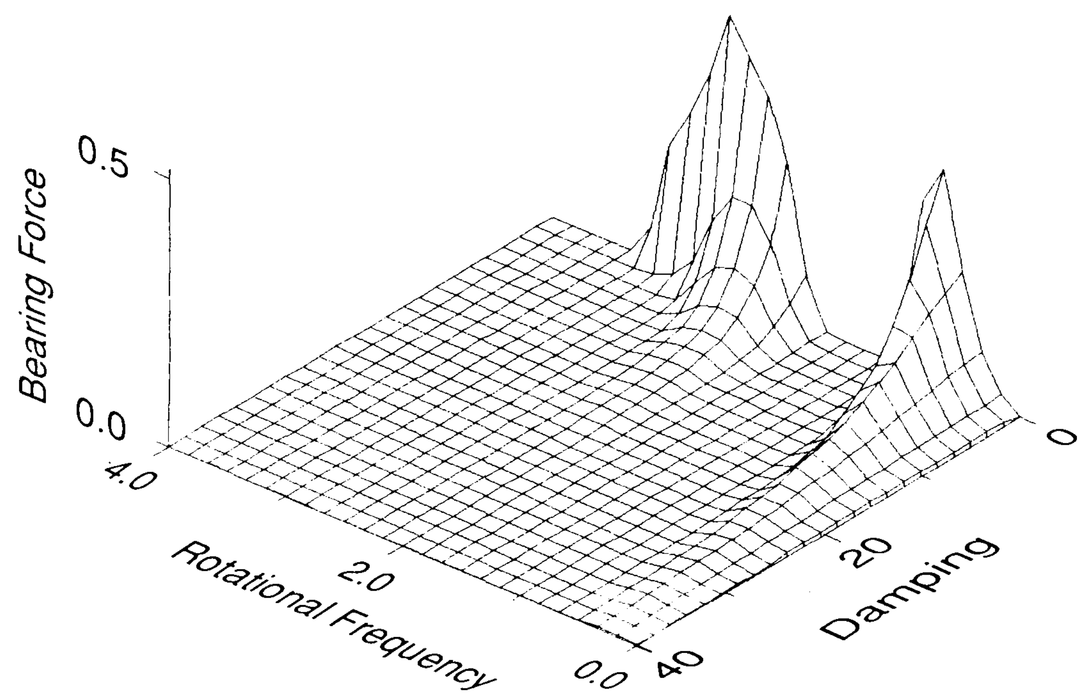

Figure 11: Minimum notch gain at each nondimensional operating speed as a function of nondimensional bearing damping ($\overline{M} = 0.5$, $\zeta_d = 0.1$)

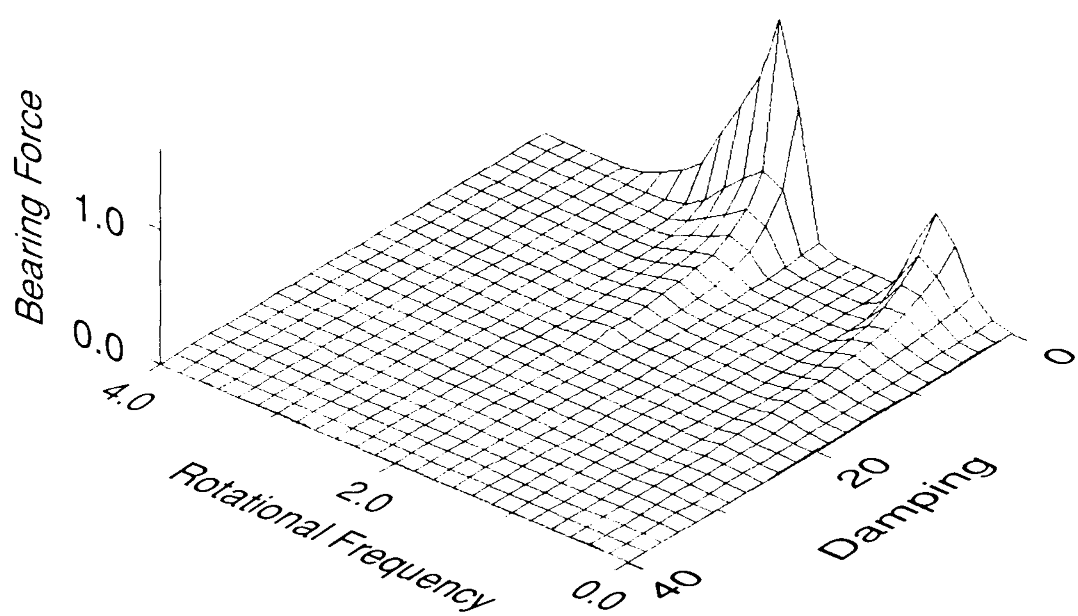

Figure 12: With notch filter control: Nondimensional transmitted synchronous force at each nondimensional operating speed as a function of nondimensional bearing damping ($\overline{M} = 0.5$, $\zeta_d = 0.1$)

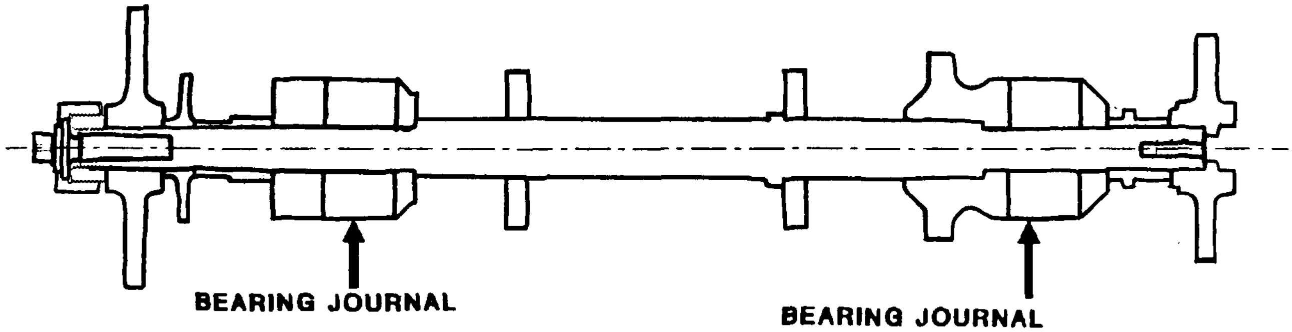

Figure 13: High speed rotor for model aircraft compressor

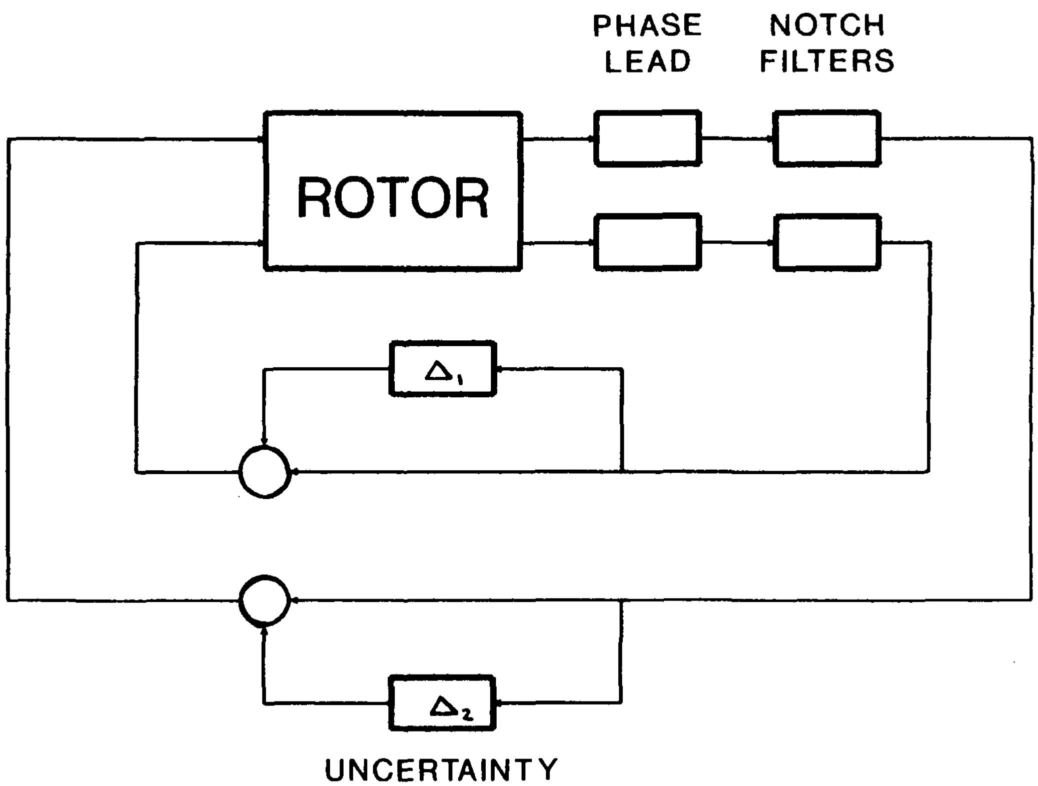

Figure 14: Uncertainty elements in feedback path

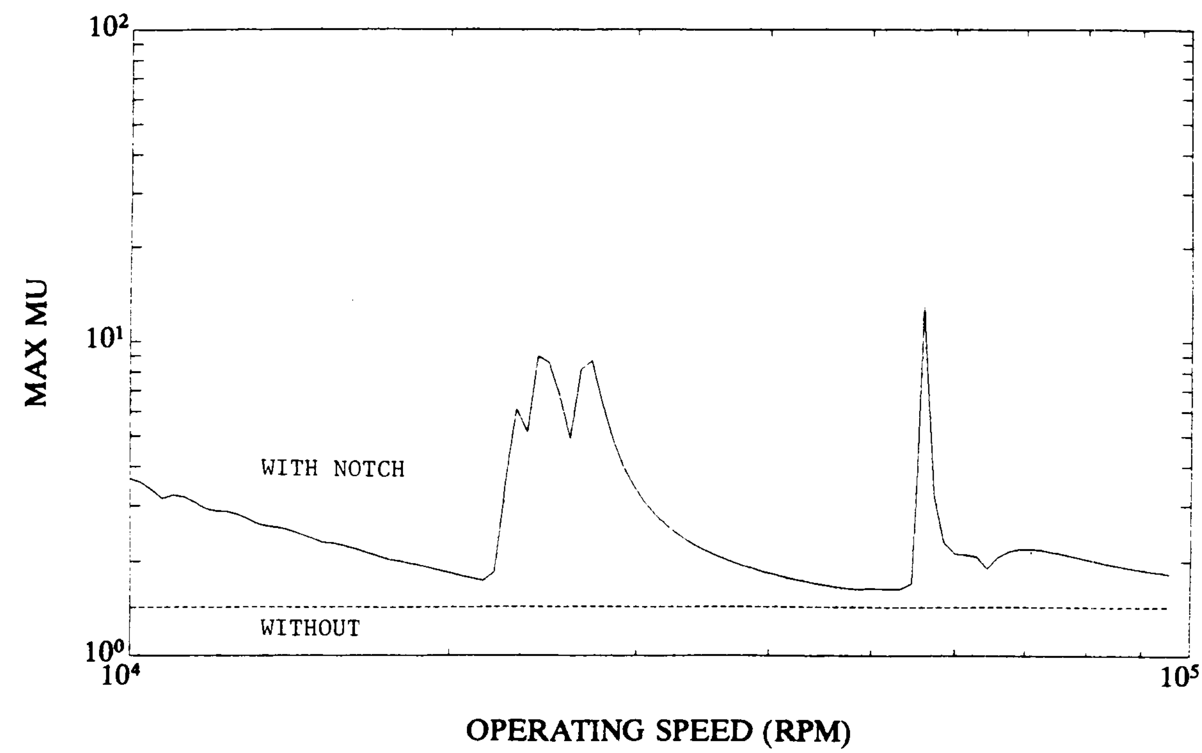

Figure 15: Maximum structured singular value with and without notch filters as a function of operating speed (notch gain = 0.1)

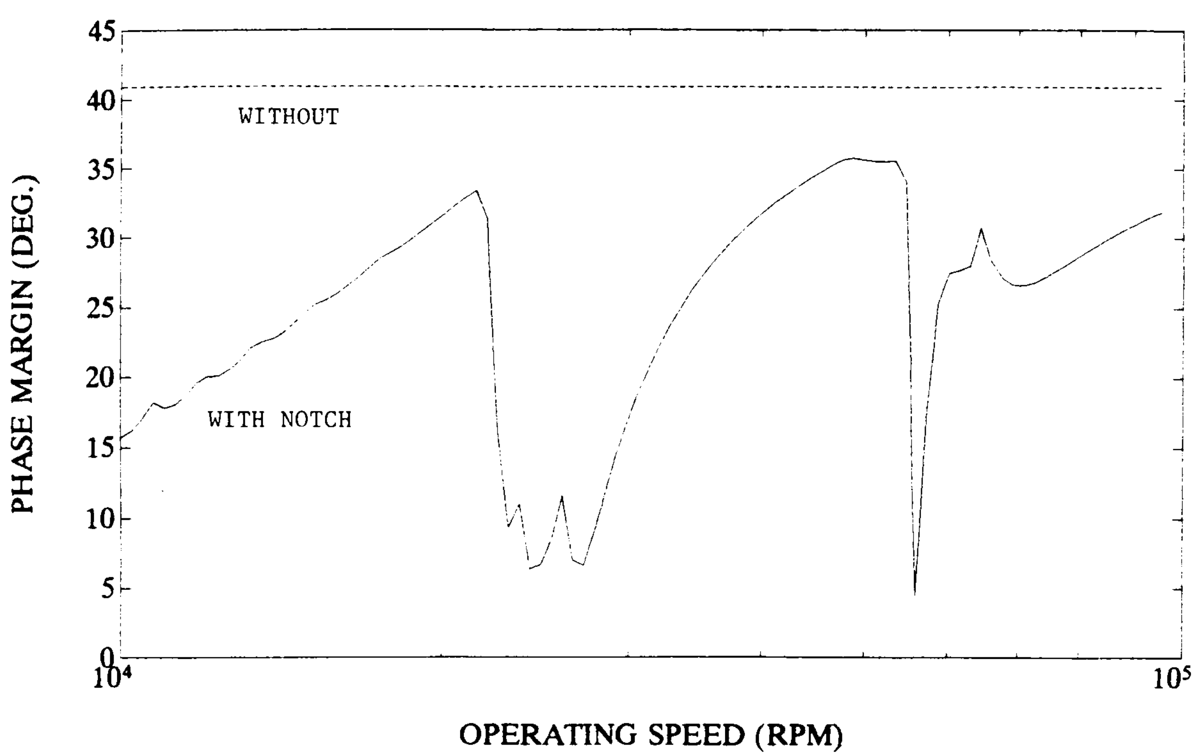

Figure 16: Guaranteed Phase margin with and without notch filters as a function of operating speed (notch gain = 0.1)

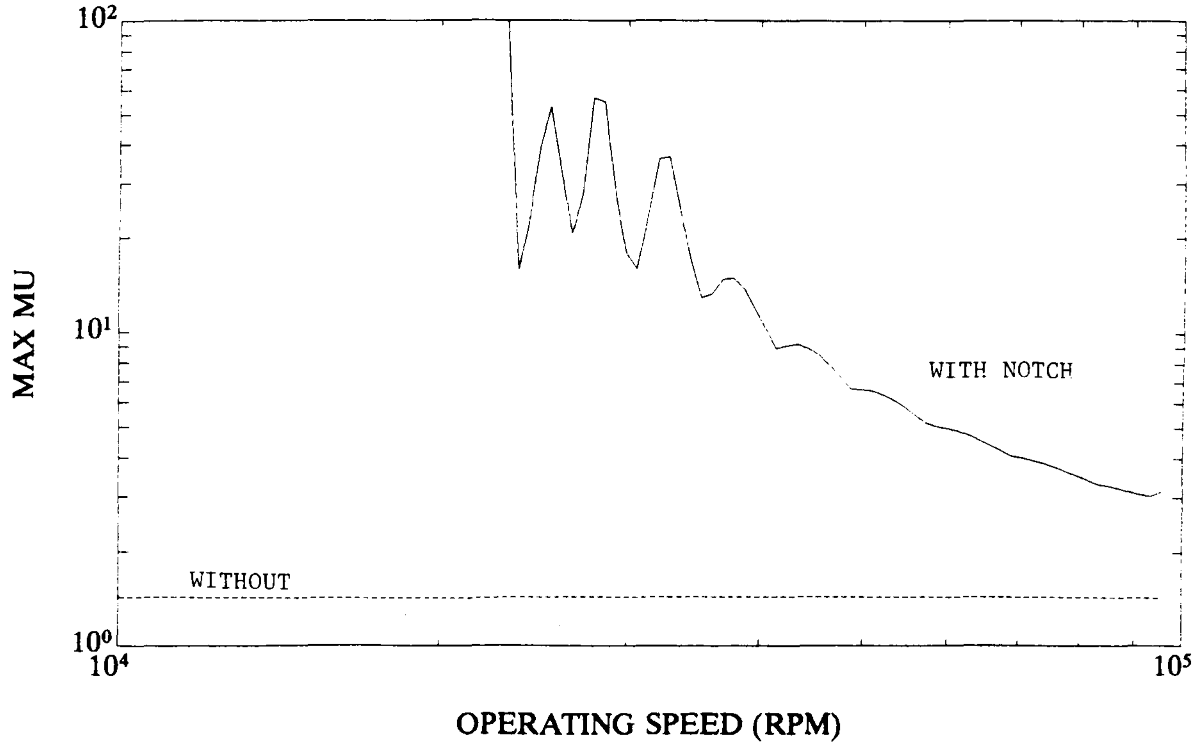

Figure 17: Maximum Structural singular value with and without notch filters as a function of operating speed (notch gain = 0.01)

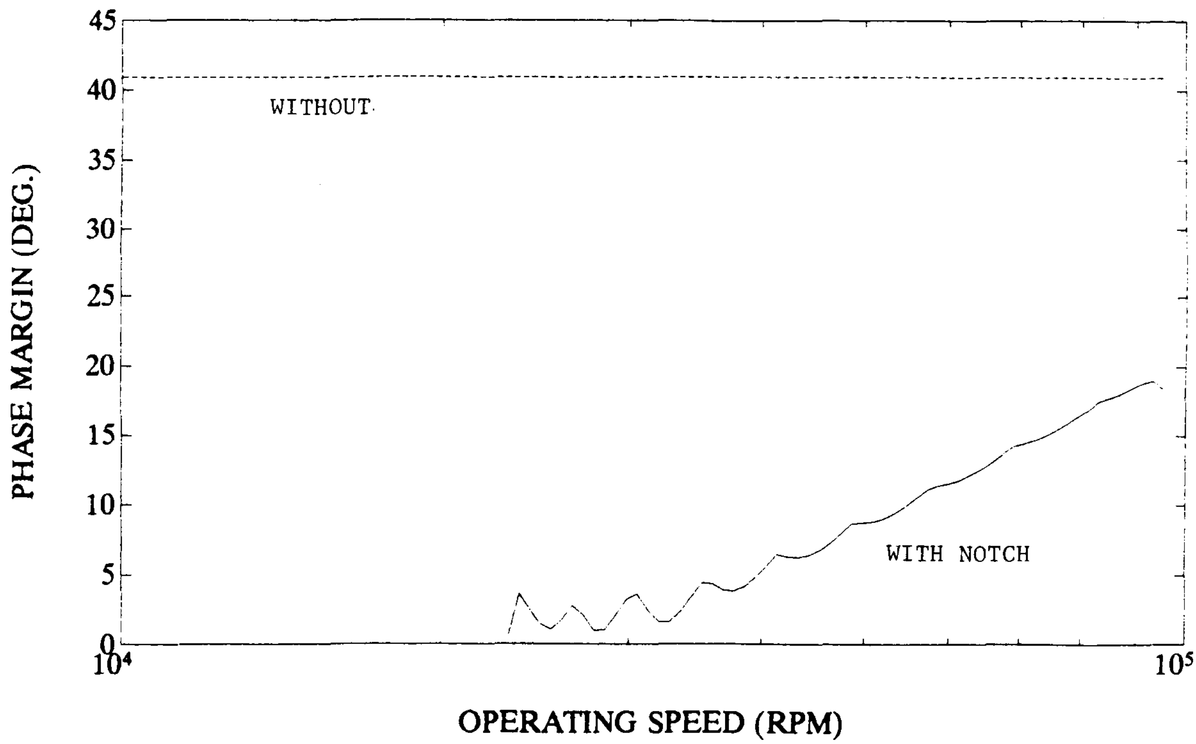

Figure 18: Guaranteed Phase Martin with and without notch filters as a function of operating speed (notch gain = 0.01)